Surface Science 606 (2012) 1345–1349

Contents lists available at SciVerse ScienceDirect

Surface Science

journal homepage: www.elsevier.com/locate/susc

Interaction of HNCO with Au(111) surfaces

A.P. Farkas, A. Berkó, F. Solymosi *

Reaction Kinetics Research Group, University of Szeged, P.O.Box 168, H-6701 Szeged, Hungary

ARTICLE INFO

Article history:
Received 22 February 2012
Accepted 25 April 2012
Available online 5 May 2012

Keywords:
HNCO
Au(111) surface
NCO surface species
NO + CO reaction
HREEL spectroscopy

ABSTRACT

The surface chemistry of isocyanic acid, HNCO, and its dissociation product, NCO, was studied on clean, O-dosed and Ar ion bombarded Au(111) surfaces. The techniques used are high resolution energy loss spectroscopy (HREELS) and temperature-programmed desorption (TPD). The structure of Ar ion etched surface is explored by scanning tunneling microscopy (STM). HNCO adsorbs molecularly on Au(111) surface at 100 K yielding strong losses at 1390, 2270 and 3230 cm^{-1}. The weakly adsorbed HNCO desorbs in two peaks characterized by $T_p = 130$ and 145 K. The dissociation of the chemisorbed HNCO occurs at 150 K to give NCO species characterized by a vibration at 2185 cm^{-1}. The dissociation process is facilitated by the presence of preadsorbed O and by defect sites on Au(111) produced by Ar ion bombardment. In the latter case the loss feature of NCO appeared at 2130 cm^{-1}. Isocyanate on Au(111) surface was found to be more stable than on the single crystal surfaces of Pt-group metals. Results are compared with those obtained on supported Au catalysts.

1. Introduction

Since the discovery and subsequent studies of the formation of NCO surface complex during the catalytic reaction of NO + CO on supported Pt metals [1–8], a huge amount of work has been published on its chemistry. Despite the extensive studies, there is still a controversy concerning the location and the role of NCO formed in the catalytic reduction of NO with CO and with hydrocarbons. The use of HNCO as a source of NCO species, however, provided an excellent possibility to produce NCO in high concentration on the surfaces of solids even at low temperature and to establish its bonding, stability and reactions. The most important findings are as follows: (i) NCO surface species developed in the catalytic reduction of NO is formed on the metals, but after its formation it migrates onto the supports, where it is stabilized [9–13]. This spillover process was first clearly demonstrated in the case of Rh/SiO_2 [12], (ii) the position of the absorption band of NCO species in the IR spectra varies with the nature of oxidic supports (Al_2O_3, MgO, TiO_2, CeO_2, ZSM-5) and fell in the range of 2210–2315 cm^{-1} [7–10], (iii) as was revealed by the studies performed on metal single crystals in UHV, the characteristic vibration of NCO bonded to the metals is at 2170–2190 cm^{-1}, which is almost independent of the nature of the metals [14–26], (iv) in contrast to the NCO attached to the oxides, isocyanate on the metals is a rather unstable species, and decomposes completely around 300–330 K [14–26]. Theoretical calculation using the density functional formalism (DFT) disclosed more details on the adsorbate–substrate interaction on different sites of metals and greatly contributed to the better understanding of the chemistry of NCO on catalyst surfaces [27–30].

Recently it was reported that not only the Pt metals are active for NO destruction, but Au nanoparticles on titania also catalyze the NO + CO reaction even at lower temperatures [31]. Initial FTIR studies failed to identify the formation of NCO [32,33], which led to a proposal of a different reaction mechanism compared to that occurring on Pt metals. More extensive studies, however, disclosed that NCO surface complex does form on supported Au catalyst in the high temperature reduction of NO with CO [34,35].

The primary aim of the present study is to produce NCO species on Au(111) surface free of support by the dissociation of HNCO and establish its chemistry. Besides the clean Au(111), the interaction of HNCO will be examined with ion bombarded and oxygen-dosed Au(111) surfaces. It is known that low energy ion bombardment generates significant structural alterations ranging from adatoms to vacancies, which lead to the increased reactivity of the surface [36–41]. On the other hand adsorbed O adatoms on Au(111) can also enhance its reactivity towards chemisorption of different molecules [42–44].

2. Experimental

The Au(111) crystal used in this work was a product of MaTeck GmbH, purity 99.999%. It was secured to a Mo plate, which was connected via a copper block directly to a liquid nitrogen reservoir. Initially the sample was cleaned by repeated cycles of Ar^+ sputtering (typically 2 kV, 1×10^{-7} mbar Ar, 300 K, 10 μA for 10–30 min) and annealing to 850–1000 K until no contaminations were detected by AES. The sample was heated with a tungsten filament situated at the back of the sample from 100 to 900–1000 K. Its temperature was

* Corresponding author. Fax: +36 62 544 106.
E-mail address: fsolym@chem.u-szeged.hu (F. Solymosi).

0039-6028/$ – see front matter © 2012 Elsevier B.V. All rights reserved.
doi:10.1016/j.susc.2012.04.025

monitored by a chromel-alumel thermocouple pressed into a hole drilled into the side of a crystal and was controlled with a feedback circuit to provide a linear heating rate of ca. 2 K/s. Gases were dosed through a 0.1 mm diameter capillary that terminated 2 cm from the sample. The local pressure at the sample was about 10^{-7} mbar during dosing. The dosing temperature was ~95–100 K unless otherwise noted.

In the preparation of ion bombarded surface we followed the method described before [36,37]. The cleaned Au(111) surface was etched for 10 min with 2 keV Ar^+ ions either at room temperature and/or after cooling to ~100 K. The angle of incidence of the Ar^+ ions was 45°, and the ion gun delivered a current density of 10 μA/cm^2. Oxygen deposition was carried out by the method described by Friend et al. [42]. Au sample was exposed to NO_2 at 100 K for 1–5 min, which resulted in a multilayer NO_2. Afterwards the sample was biased to +100 V and exposed to an electron source of the mass spectrometer filament with an emission current of 2 mA for 1 min. Upon heating the adsorbed layer to 300 K the weakly adsorbed NO_2 desorbed and the adsorbed oxygen atoms remained on the surface. Repeating this procedure several times the surface concentration of adsorbed O atoms can be increased. As was reported by Friend et al. [42] oxygen desorbed from Au(111) with a $T_p = 550$ K, the amount of O_2 desorbed allows to determine the approximate coverage of adsorbed O. The preparation of HNCO was described in our previous papers in detail [9].

The experimental work was performed in a two-level UHV chamber with a routine base pressure of 5×10^{-10} mbar produced by turbomolecular pump. The chamber was equipped with facilities for AES, HREELS and TPD. The HREEL spectrometer (LK, ELS 3000) is situated in the lower level of the chamber and has a resolution of 20–40 cm^{-1} (FWHM). The count rates in the elastic peak were typically in the range of 1×10^4 to 1×10^5 counts-per-second (cps). All spectra reported were recorded with primary beam energy of 6.5 eV and at an incident angle of 60° with respect to the surface normal in the specular direction.

An ultrahigh vacuum compatible, room temperature scanning tunneling microscope (WA Technology, U.K.) was used for the study of the nanoscale morphological changes of Au(111) surface induced by Ar^+ bombardment. It was installed in a separate UHV chamber capable also for Auger-electron spectroscopy (AES). The latter technique was substantially important to check the cleanliness of the probe, although, the appearance of the characteristic "herring-bone" decoration of the large (111) terraces indicated also clearly the purity of the gold surface [41]. The STM images were taken in the so called constant current mode with an electrochemically etched tungsten tip. For the calibration of the STM head, a routinely examined rutile TiO_2(110) surface served. The STM images of 256×256 pixels were typically recorded at a bias of +1 V on the sample and an average tunneling current of approximately 10 nA. The recorded images were analyzed with commercial SPIP image processor software.

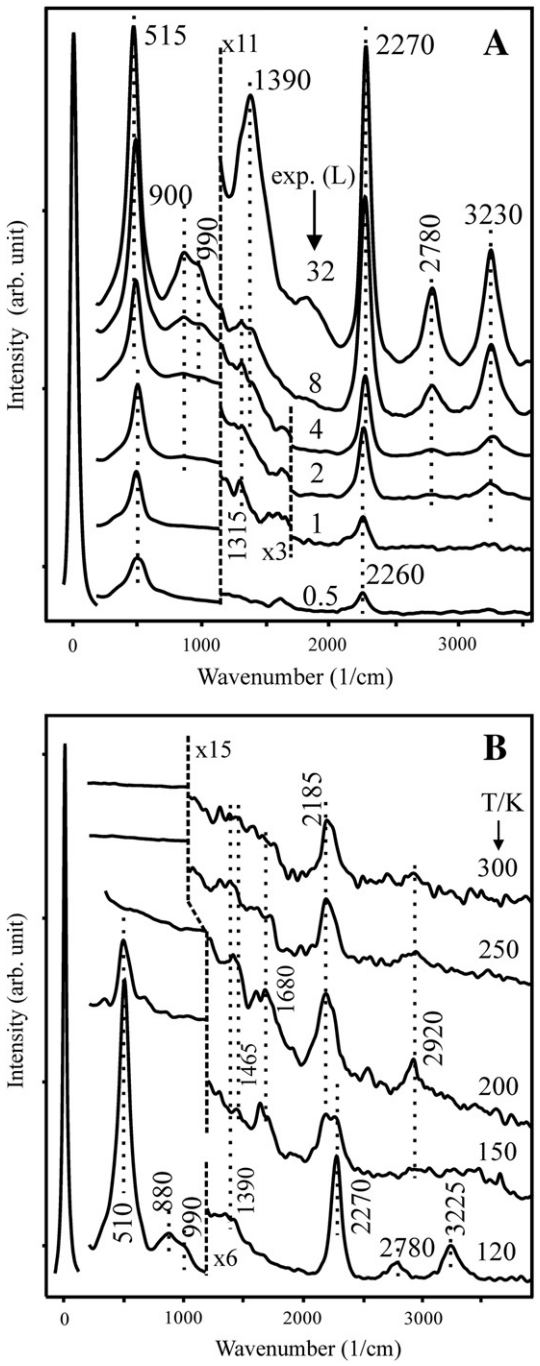

Fig. 1. Effects of HNCO exposure on the HREEL spectra of untreated Au(111) at ~100 K (A), and subsequent annealing (B) (exposure of HNCO was 8.0 L).

3. Results and discussion

3.1. Clean Au(111) surface

HREELS spectra of Au(111) at different HNCO exposures at ~100 K are presented in Fig. 1A. The adsorption of HNCO caused the appearance of several losses at 515, 900, 990, 1390, 2270, 2780 and 3230 cm^{-1}, which became more intense with the increase of the HNCO exposure. The most important spectral feature is the loss at the 2270 cm^{-1}, which is due to the asymmetric stretching of molecularly adsorbed HNCO. The position of this loss was found to be independent of the surface coverage of adsorbed HNCO. The same feature was observed in the HREEL spectra of HNCO adsorbed on Pt(111) [14] and Rh(111) [45], whereas the RAIRS disclosed a coverage dependence on Pt(111) surface [25]. The symmetric stretch, which is much weaker than the previous one, can be detected at 1390 cm^{-1}. The peak at 3230 cm^{-1} is the NH stretching. We assume that the loss at 2920 cm^{-1} and that at 2780 cm^{-1} are the overtones of the peaks at 1465 cm^{-1} and at 1390 cm^{-1} [46]. The vibration at 1615–1620 cm^{-1}, which appears sometimes, is very likely the result of the adsorption of H_2O from the background. The positions of the vibration losses observed and their possible assignment are presented in Table 1, which also contains the results obtained for other metal surfaces.

Annealing the adsorbed layer resulted in attenuation of vibration loss at 2270 cm^{-1}, and in the development of new spectral feature at 2185 cm^{-1} at around 150 K (Fig. 1B). This vibration loss was detectable up to ~430 K. The loss at 2170–2185 cm^{-1} was also

Table 1
Frequencies (cm^{-1}) and assignment of the fundamental vibrations of vapor, solid and adsorbed HNCO.

Assignment	Vapor	Solid	Pt(111) [14]	Rh(111) [15]	Au(111) [present study]
ν_1 (a′) ν(NH)	3531	3133	3240	3373; 3240	3230
$2\nu_3$					2780
ν_2 (a′) ν_a(NCO)	2274	2246	2270	2277	2270
$\nu_4+\nu_6$	1480	1460	1450	1444	
$\nu_4+\nu_5$	1371	1377		1419	
ν_3 (a′) ν_s(NCO)	1327	1326	1360	1322	1390
ν_4 (a′) δ(NCO)	797	–	870		900
ν_5 (a′) hindered rotation	572	–	530		515
ν_6 (a″)	670	–			

Note. Data for HNCO in vapor and solid phases were taken from Ref. [15] $\nu_4+\nu_6$; $\nu_4+\nu_5$ correspond to the combination of fundamental vibrations.

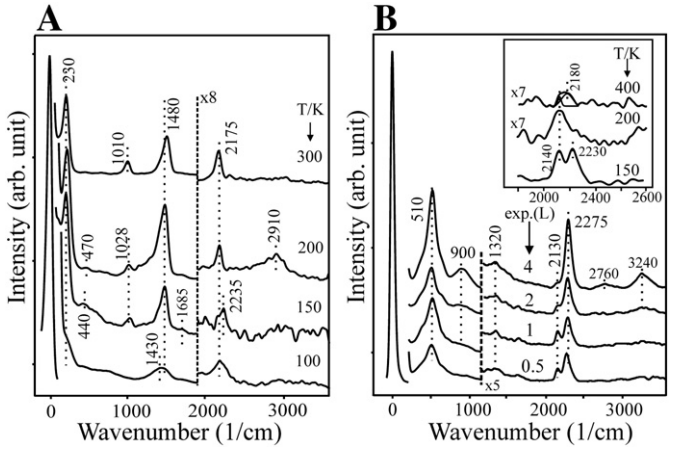

Fig. 3. Effects of preadsorbed oxygen (Θ_O ~0.3) (A) and Ar ion bombardment (B) on the HREEL spectra of HNCO on Au(111) at ~100 K. In the segment the effect of annealing is presented.

observed by different vibration spectroscopic studies on other metal single crystal surfaces, and was attributed to the asymmetric stretching of surface NCO species [14–24]. Accordingly adsorbed HNCO undergoes dissociation on Au(111) surface around 150 K, practically at the same temperature as the desorption of HNCO (Fig. 2A),

$$HNCO_{(a)} = NCO_{(a)} + H_{(a)} \quad (1)$$

although this reaction was not expected to occur on the relatively inert Au(111). The disappearance of the N – H stretching and the attenuation of the 510 and 2780 cm^{-1} vibrations characteristic also to molecular HNCO, is in good harmony with the occurring of the dissociation process. This reaction proceeded easily on Pt metals [14–25], but on Cu(111) it required the presence of preadsorbed O atoms [45]. However, we cannot exclude the possibility that the method (EEL spectroscopy in the electronic range), applied earlier in the case of Cu(111) was much less sensitive than the HREEL spectroscopy used at the present.

TPD spectra following the HNCO adsorption on Au(111) at different exposures are displayed in Fig. 2A. At lower exposure, up to 1.0 L HNCO desorbs with a peak, $T_p = 145$ K. No alteration occurs in this value with the increase of the exposure, which suggests a first order desorption. The activation energy of this process calculated from the peak temperature is 36 kJ/mol. The activation energy for desorption processes was calculated using the Redhead formula. Above 1.0 L exposure another peak is developed with $T_p = 130$ K, which cannot be saturated. We attribute this peak to the desorption of a condensed layer. We obtained 32 kJ/mol for the activation energy of this process. At higher temperatures, we also observed HNCO desorption with Tp ~230–210 K (Fig. 2A). We attribute this peak to HNCO molecules produced after recombination of $H_{(a)}$ and $NCO_{(a)}$ species. When we searched after reaction products, we detected weak signals of amu 28 and 12 at T_p~480 K (Fig. 2B), which we attribute to the release of CO and N_2 formed in the decomposition of NCO bonded to Au

$$NCO_{(a)} = CO_{(g)} + N_{(a)} \quad (2)$$

$$2N_{(a)} = N_{2(g)} \quad (3)$$

As CO does not remain adsorbed on clean Au(111) above 250 K [47], the above peak temperature indicates the stability of NCO on Au(111) surface. We may also assume that the N atoms formed in the process described by Eq. (2), also recombine after their production. We did not observe peak at M(42) due to the desorption of NCO. This is in harmony with the results obtained in previous papers.

These results confirm the assignment and the interpretation of FTIR spectra obtained following the NO + CO reaction on supported Au catalysts [34,35]. Adsorption of NO + CO gas mixture on Au/SiO_2 at 473–523 K produced an intense absorption band at ~2190 cm^{-1}, together with a weak band at 2305 cm^{-1}. After longer reaction time and/or at higher temperature the 2190 cm^{-1} band attenuated and

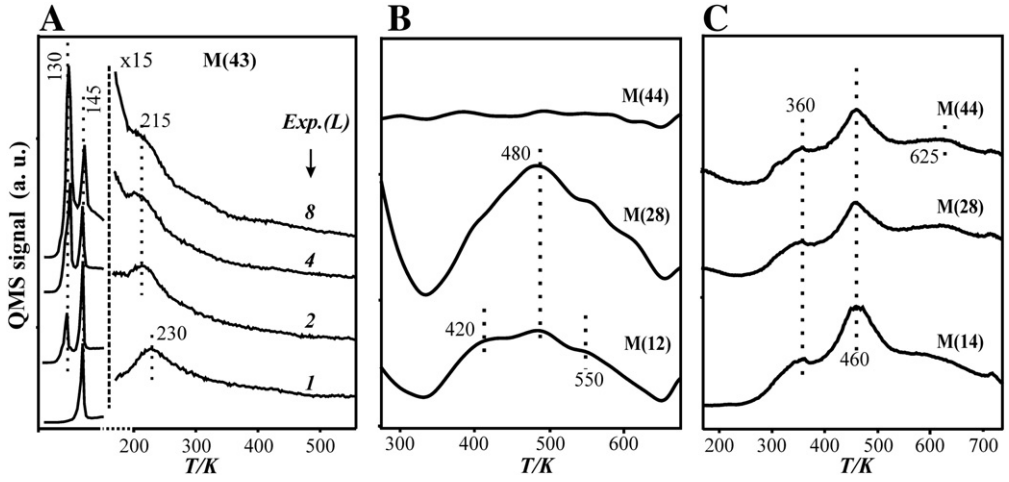

Fig. 2. TPD spectra for HNCO at different exposures at 100 K (A) and for its decomposition products released from untreated Au(111) (B) and from O-dosed Au(111) surface (C). $T_a \approx 110$ K. The approximate coverage of adsorbed O is 0.2–0.3.

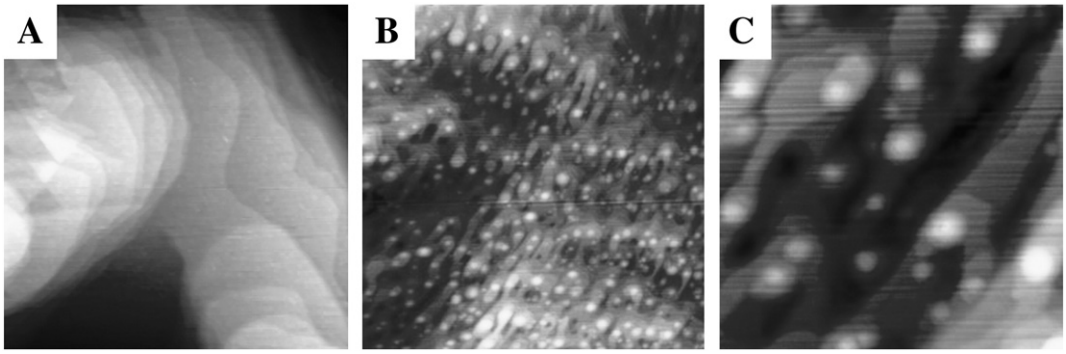

Fig. 4. STM images recorded on untreated Au(111) (A) and on an Ar^+ sputtering modified Au(111) at room temperature for 10 min (3 keV, 5 μA/cm^2) (B and C). The size of the images: (A, B) 400×400 nm^2, (C) 100×100 nm^2. The STM images were recorded at a bias of +1 V on the sample and an average tunneling current of app. 10 nA.

disappeared. At the same time the band at 2305 cm^{-1} due to Si-NCO strengthened and finally dominated the spectra. This feature is in agreement with the results obtained following the dissociative adsorption of HNCO on supported Au catalyst [34,35]. On the Au/TiO_2 and Au/SiO_2 samples the absorption band at 2180–2190 cm^{-1} due to Au-NCO was present even at 523 K.

3.2. Oxygen-dosed Au(111)

In the subsequent measurements we examined the adsorption of HNCO on Au(111) containing adsorbed O atoms. HREEL spectra are presented in Fig. 3A. The vibration loss at 2175 cm^{-1} due to NCO species already appeared at 100 K, e.g. at considerably lower temperatures than on a clean Au(111) sample. This result clearly suggests that O atoms on Au(111) surface promote the dissociation of HNCO, very likely due to the formation of OH species

$$HNCO_{(g)} + O_{(a)} = NCO_{(a)} + OH_{(a)} \quad (4)$$

We could not find unambiguous evidences for the formation of $OH_{(a)}$ on the HREEL spectra which possibly caused by the orientation of the hydroxyl species or by the very low surface concentration.

By means of TPD measurements we detected the evolution of CO_2 with T_p = 360 and 460 K in addition to that of CO and N_2 (Fig. 2C). This suggests that NCO reacted with preadsorbed O

$$NCO_{(a)} + O_{(a)} = CO_{2(g)} + 1/2N_{2(g)} \quad (5)$$

yielding CO_2. We can explain the attendance of this double desorption peak possibly by the presence of different kind of adsorption sites available on the reconstructed Au(111) surface. As CO_2 is not bonded to Au(111) surface above 200 K [48], its high Tp value for the evolution of CO_2 indicates the reaction temperature of the oxidation process.

In addition to the above described effect it should be taken into account that the generation of atomic oxygen using electron-induced dissociation of NO_2 induces restructuring of Au(111) herringbone structure. This is accompanied by the formation of small gold island and/or serrated step edge due to the release of gold atoms at the expense of herringbone elbow sites (dislocation sites) [42]. This feature can also contribute to the enhanced reactivity toward HNCO adsorption and dissociation. But this surface modification is much less than that caused by Ar^+ bombardment.

3.3. Argon ion bombarded Au(111)

The interaction of HNCO and its chemistry were also investigated on Ar ion bombarded Au(111) surface. First we examined the structural changes occurred on the Au(111) sample. In Fig. 4 we present scanning tunneling (STM) images recorded on a well ordered (annealed) and an Ar^+ bombardment modified Au(111) surface. The intact surface exhibits characteristically large, atomically smooth terraces, with monatomic steps between the terraces (Fig. 4A). The corrugation (height difference between the highest and lowest points of the imaged area) was approximately 4–5 nm for an image size of 400×400 nm^2. This parameter does not vary significantly on the effect of an Ar^+ bombardment of 3 keV ion energy and 5 μA/cm^2 ion current density at room temperature for 10 min (Fig. 4B), however, the main characteristic of the original morphology changes dramatically. Instead of extended monoatomic terraces, parallel running hills with a periodicity of approximately 20 nm and individual dot-like features of 10–15 nm diameter can be seen everywhere. The small scale corrugation increases significantly, mainly due to the outrising dots which consist usually of 4–6 rising steps (Fig. 4C). This STM image of 100×100 nm^2 also shows parallel hills running in the diagonal direction of the region. The front line of this surface wave is probably perpendicular to the direction of the generating Ar^+ beam. As a conclusion, these STM measurements reveal that ion bombardment increased the density of steps significantly whereas the typical terrace width was considerably reduced, especially at the side walls of the pits and mounds. Interestingly, although the ion bombardment transformed the flat terraces into a net of pits and mounds, the determining features are still (111) terraces with a strongly reduced average lateral size. According to the quantitative analysis of several images taken on freshly sputtered surfaces, we concluded that the sputtering increased the density of Au atoms located at step edge sites by almost 2 orders of magnitude (up to 10^{14} step atoms/cm^2). It can obviously be assumed that this tendency is even more evident when the sputtering is performed deep below room temperature. It appears clearly that Ar ion bombardment increases significantly the density of steps on Au(111) surface, whereas the typical terrace width is considerably reduced. Note that annealing the etched sample at 500 K for 1–2 min leads a complete restoration of the original surface ordering.

Exposures of the etched Au(111) surface to HNCO at 100 K resulted qualitatively in the same spectral features as in the case of the untreated sample. The intensity of the loss at 2275 cm^{-1} (Fig. 3B) due to asymmetric stretching of molecularly bonded HNCO was, however, appreciably larger than that measured on an untreated surface at the same exposure. This can be attributed to the higher active surfaces area of the Ar^+ bombarded sample. A more important difference is that the loss feature at 2185 cm^{-1} observed on an unperturbed surface is missing. Instead, a new loss at 2130 cm^{-1} developed. Its intensity somewhat enhanced up to 150 K, and attenuated at higher temperatures. On the basis of previous interpretation, we may assume that this peak belongs to NCO formed in the dissociation of adsorbed HNCO (Eq. (1)). Its appearance at 100 K can be attributed to the high concentration of the low coordinated atoms generated by the sputtering of Au(111) surface, which are significantly more active than the highly coordinated terrace atoms. The lower position of the NCO vibration is probably the result of different electronic structure of the new sites. An alternative explanation could be that this loss is not

due to NCO, but rather due to CN species formed in the breaking of the C – O bond in the NCO

$$NCO_{(a)} = CN_{(a)} + O_{(a)} \quad (6)$$

This new reaction channel was not observed before following the HNCO adsorption on any metal [14–23], but was recently reported to occur in the interaction of HNCO with Pt(111) [24]. The existence of this route was supported by the formation of NO on the initially oxygen-free surface, and by the release of HCN. In the present case, however, there was no sign of the presence of the loss at 2170–2180 cm^{-1} due to NCO, and we could not detect the desorption of either NO or HCN. Therefore we incline to think that the vibration at 2130 cm^{-1} is the asymmetric stretching of NCO formed in the dissociation of HNCO on the very active sites of the etched Au(111) surface.

3.4. Comparison of the behavior of Au with that of Pt metals

The results unambiguously show that NCO species exists on Au surface. The position of the asymmetric stretching of NCO agrees well with that determined on Pt metal surfaces (Table 1). The chemistry of NCO on Au(111) surface, however, basically differs from that observed on Pt, Pd, and Rh single crystals. In the latter cases, NCO was found to be a relatively unstable surface compound; it decomposes completely at 300–330 K [14,15,23–25]. In the present case it existed even at ~430 K. The possible reason is that there is no driving force for its decomposition as the binding energy for Au-CO and Au-N is much smaller than that on Pt metals.

A consequence of the high stability of NCO on Au metal is that it could be present in low concentration even in the catalytic reduction of NO with CO at high temperature. In other words it can function as a surface intermediate, or poisons the active sites of the Au nanoparticles. The role of NCO is possibly determined by the nature of the support. In the case of alumina support, when the spillover of NCO from Au onto Al_2O_3 is fast, the Au-NCO complex plays less role in the NO + CO reaction. In contrast applying silica as a support when the migration of NCO from Au onto SiO_2 is very slow, its existence on the Au may influence the reaction. From this point of view it would be interesting to compare the catalytic activity of Au/Al_2O_3 and Au/SiO_2 in the NO + CO reaction. Experiments are in progress to examine these considerations.

4. Conclusions

(i) HNCO adsorbs molecularly on pure Au(111) surface at ~100 K and undergoes dissociation to NCO and H around 150 K. NCO species formed on Au surface is stable up to ~430 K, e.g. at much higher temperatures than on Pt metals.

(ii) The characteristic vibration of NCO species bonded to Au(111) is at 2180–2190 cm^{-1}, which suggests that the absorption bands observed at higher wavenumbers for supported Au catalyst during the NO + CO reaction are due to NCO bonded not to the Au, but rather to the oxidic supports.

(iii) Preadsorbed oxygen and bombardment of the Au(111) surface with Ar ions enhanced the amount of weakly adsorbed HNCO, and induced the formation of NCO complex even at 100 K.

(iv) Scanning tunneling microscopic measurements revealed the appearance of a large number of steps on the Ar ion treated Au surface, which are probably responsible for the enhanced reactivity towards HNCO dissociation.

Acknowledgments

This work was supported by the grant OTKA under contract number K 81517 and K 69200.

References

[1] M.L. Unland, J. Phys. Chem. 77 (1973) 1952; M.L. Unland, J. Catal. 31 (1973) 459.
[2] J.W. London, A.T. Bell, J. Catal. 31 (1973) 96.
[3] F. Solymosi, J. Sárkány, React. Kinet. Catal. Lett. 3 (1975) 297.
[4] M.F. Brown, R.D. Gonzalez, J. Catal. 44 (1976) 477.
[5] A.A. Davydov, A.T. Bell, J. Catal. 49 (1977) 345.
[6] F. Solymosi, J. Kiss, J. Sárkány, Proceedings, 7th International Vacuum Congress and 3rd International Conference on Solid Surfaces, Vienna, 1977, p. 819.
[7] F. Solymosi, L. Völgyesi, J. Sárkány, J. Catal. 54 (1978) 336.
[8] F. Solymosi, J. Sárkány, Appl. Surf. Sci. 3 (1979) 68.
[9] F. Solymosi, T. Bánsági, J. Phys. Chem. 83 (1979) 552.
[10] J. Raskó, F. Solymosi, J. Catal. 71 (1981) 219.
[11] D. Lorimer, A.T. Bell, J. Catal. 59 (1979) 223.
[12] T. Bánsági, J. Raskó, F. Solymosi, Proceedings, International Symposium on Spillover of Adsorbed Species, Lyon, Elsevier, Amsterdam, 1983, p. 109.
[13] W.C. Hecker, A.T. Bell, J. Catal. 85 (1984) 389.
[14] R.J. Gorte, L.D. Schmidt, B.A. Sexton, J. Catal. 67 (1981) 387.
[15] J. Kiss, F. Solymosi, J. Catal. 179 (1998) 277.
[16] K.L. Kostov, P. Jacob, H. Rauscher, D. Menzel, J. Phys. Chem. 95 (1991) 7785.
[17] K.L. Kostov, H. Rauscher, D. Menzel, Surf. Sci. 287/288 (1993) 283.
[18] J.H. Miners, A.M. Bradshaw, P. Gardner, Phys. Chem. Chem. Phys. 1 (1999) 4909.
[19] E. Ozensoy, C. Hess, D.W. Goodman, J. Am. Chem. Soc. 124 (2002) 8524.
[20] H. Celio, K. Mudalige, P. Mills, M. Trenary, Surf. Sci. 394 (1997) L168.
[21] C. Hess, D.W. Goodman, E. Ozensoy, J. Phys. Chem. B 107 (2003) 2759.
[22] C. Hess, E. Ozensoy, D.W. Goodman, J. Phys. Chem. B 108 (2004) 14181.
[23] R. Németh, J. Kiss, F. Solymosi, J. Phys. Chem. C 111 (2007) 1424.
[24] E. Herceg, J. Jones, K. Mudiyanselage, M. Trenary, Surf. Sci. 600 (2006) 4563.
[25] J.E. Jones, M. Trenary, J. Phys. Chem. C 112 (2008) 20443.
[26] F. Solymosi, A. Berkó, T.I. Tarnóczi, Appl. Surf. Sci. 18 (1984) 233.
[27] R.M. Ferullo, N.J. Castellani, J. Mol. Catal. A: Chem. 221 (2004) 155.
[28] G.R. Garda, R.M. Ferullo, N.J. Castellani, Surf. Sci. 598 (2005) 57.
[29] P.G. Belelli, M.M. Branda, G.R. Garda, R.M. Ferullo, N.J. Castellani, Surf. Sci. 604 (2010) 442.
[30] P.G. Belelli, G.R. Garda, R.M. Ferullo, Surf. Sci. 605 (2011) 1202 and references therein.
[31] A. Uleda, M. Haruta, Gold Bull. 32 (1999) 3.
[32] J.Y. Lee, J. Schwank, J. Catal. 102 (1986) 207.
[33] M.A. Debeila, N.J. Coville, M.S. Scurrell, G.R. Hearne, Catal. Today 72 (2002) 79.
[34] F. Solymosi, T. Bánsági, T. Süli Zakar, Catal. Lett. 87 (2003) 7.
[35] F. Solymosi, T. Bánsági, T. Süli Zakar, Phys. Chem. Chem. Phys. 5 (2003) 4724.
[36] W.L. Chan, E. Chason, J. Appl. Phys. 101 (2007) 121301 and references therein.
[37] Z. Pászti, O. Hakkel, T. Keszthelyi, A. Berkó, N. Balázs, I. Bakó, L. Guczi, Langmuir 26 (2010) 16312.
[38] L. Savio, L. Vattuone, M. Rocca, Phys. Rev. B 67 (2003) 045406.
[39] O. Skibbe, D. Vogel, M. Binder, A. Pucci, T. Kravchuk, L. Vattuone, V. Venugopal, A. Kokalj, M. Rocca, J. Chem. Phys. 131 (2009) 024701.
[40] A. Politano, G. Chiarello, J. Phys. D: Appl. Phys. 43 (2010) 085302.
[41] J.V. Barth, H. Brune, G. Ertl, R. Behm, J. Phys. Rev. B 42 (1990) 9307.
[42] X. Deng, B.K. Min, A. Guloy, C.M. Friend, J. Am. Chem. Soc. 127 (2005) 9267.
[43] J. Gong, B. Mullins, Acc. Chem. Res. 42 (2009) 1063 and references therein.
[44] S.A.C. Carabinerio, B.E. Nieuwenhuys, Gold Bull. 43 (2010) 252.
[45] F. Solymosi, J. Kiss, Surf. Sci. 104 (1981) 181.
[46] M. Surman, F. Solymosi, R.D. Diehl, P. Hofmann, D.A. King, Surf. Sci. 146 (1984) 135.
[47] W.-L. Yim, T. Nowitzki, M. Necke, H. Schnars, P. Nickut, J. Biener, M.M. Biener, V. Zielasek, K. Al-Shamery, T. Klüner, M. Bäumer, J. Phys. Chem. C 111 (2007) 445.
[48] A.P. Farkas, F. Solymosi, J. Phys. Chem. C 113 (2009) 19930.